

## MIXED-TYPE INHIBITION OF BOVINE LUNG ANGIOTENSIN CONVERTING ENZYME BY LISINOPRIL AND ITS DANSYL DERIVATIVE

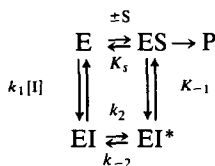
GÜLBERK UÇAR and İNCİ ÖZER\*

Department of Biochemistry, School of Pharmacy, Hacettepe University, 06100 Ankara, Turkey

(Received 13 January 1992; accepted 6 April 1992)

**Abstract**—The steady-state inhibition of bovine lung angiotensin converting enzyme (ACE; EC 3.4.15.1) by the slow-binding inhibitor lisinopril and its dansyl derivative conformed to a linear mixed inhibition model with inhibitor binding to ES as well as to E. Studied at pH 8, 35°, and using *N*-(3-[2-furyl]-acryloyl)phe-gly-gly as substrate, the approach to steady-state activity at different substrate concentrations pointed to slow isomerizations in both EI and EIS. While an inhibitory scheme involving a single I-binding site adequately accounts for the data presented, information relating to the primary structure of ACE brings up a two-site alternative which remains to be tested.

As a component of the renin–angiotensin–aldosterone system, angiotensin converting enzyme (ACE†; EC 3.4.15.1) has been a major target in the design of antihypertensive drugs [1–4]. A substantial volume of data has accumulated also with respect to the molecular and kinetic properties of the enzyme [5–19] and the gene encoding it [20]. Of particular interest from the kinetic viewpoint is the observation that some reversible inhibitors of ACE such as captopril, enalaprilat and lisinopril act as slow, tight-binding inhibitors conforming to Scheme I [21–24], where binding



Scheme I

of I to E is driven by the subsequent slow isomerization of EI to EI\*. Scheme I has been deduced from progress curves for the hydrolysis of *N*-(3-[2-furyl]acryloyl)phe-gly-gly (FAPGG) in the presence of inhibitor. Evidence for conformational changes has been obtained also in the chloride-dependent hydrolysis of Class III substrates in the absence of inhibitor [25, 26]. What follows is the result of a preliminary search for a fluorescent inhibitor which would exhibit slow-binding properties and could be used to monitor I-induced change(s) in enzyme conformation in the absence of substrate. Steady-state inhibition data obtained with bovine ACE using lisinopril and DNS-lisinopril are at variance with the simple competitive model previously proposed to account for the inhibition of rabbit lung

ACE and point to possible multiplicity in I-binding modes.

### MATERIALS AND METHODS

Lisinopril was a gift of Merck Sharp & Dohme, U.S.A. Chromatographic media were obtained from Pharmacia-LKB, Sweden. All other chemicals were from the Sigma Chemical Co., U.S.A.

ACE was partially purified from bovine lung using conventional methods: 200 g tissue was homogenized in 4 vol. of 50 mM potassium phosphate (pH 8) containing 30 mM KCl. The homogenate was centrifuged at 16,300 *g* for 60 min. The pellet was resuspended in 2.5 vol. of homogenization buffer (HB) using a Waring blender, brought to 0.1% in Triton X-100 and incubated in a 35° water bath for 1 hr. Following centrifugation at 16,300 *g* for 60 min, the Triton extract was subjected to ammonium sulfate precipitation overnight (4°, 65% saturation). The precipitate was collected by centrifugation at 27,000 *g* for 90 min, resuspended in *ca.* 70 mL HB containing 0.05% Triton-100, and cleared by centrifugation. The supernatant (60 mL) was dialyzed against 2 × 2300 mL of 20 mM potassium phosphate (pH 7) containing 0.05% Triton X-100. Particulate matter was removed by centrifugation. The supernatant was applied to a 3 × 29 cm column of DEAE-Sephadex A50 equilibrated with dialysis buffer. Elution was performed using a linear gradient (800 mL) of 0 to 0.5 M KCl in the same buffer. ACE activity eluted at 0.23 M KCl. Active fractions were pooled, dialyzed against 20 vol. of 25 mM imidazole·HCl buffer (pH 7.4) containing 0.025% Triton X-100 and 0.1 mM ZnCl<sub>2</sub> and applied to a 1.5 × 7.5 cm column of PBE 94 equilibrated with the same buffer (omitting ZnCl<sub>2</sub>). Chromatofocusing was done with PB 74 (diluted 1:8 with water, adjusted to pH 4 with HCl and supplemented with 0.025% Triton X-100). Activity was recovered in the pH range 5–4 (Fig. 1). Fractions 50–75 on the basic side were pooled, adjusted to pH 6 with 1 M Tris, and applied to the PBE 94 column equilibrated with

\* Corresponding author. Tel. (90) 4311 87 01; FAX (90) 4311 47 77.

† Abbreviations: ACE, angiotensin converting enzyme; DNS-, dansyl-; and FAPGG, *N*-(3-[2-furyl]acryloyl)phe-gly-gly.

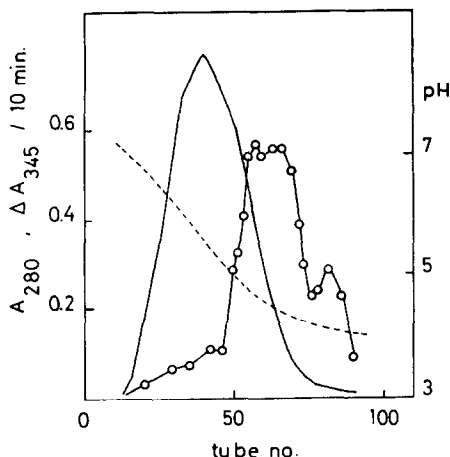


Fig. 1. Chromatofocusing of bovine lung ACE. Column dimensions,  $1.5 \times 7.5$  cm; flow rate, 20 mL/hr; fraction volume, 3 mL. Key: (—)  $A_{280}$ ; (○) activity; and (----) pH.

25 mM imidazole·HCl (pH 6)–0.025% Triton X-100. Gradient elution (0 to 0.3 M KCl; 600 mL) yielded enzyme at *ca.* 0.1 M KCl. The preparation had a specific activity of 20 U/mg, based on  $V_{\max}$  using FAPGG as substrate (see section on kinetic measurements). Protein was determined according to Bradford [27].

**Preparation of dansyl-lisinopril.** Lisinopril (17  $\mu$ mol) was dissolved in 10 mL of 50 mM NaHCO<sub>3</sub> and added to 50  $\mu$ mol solid dansyl chloride. The mixture was stirred at room temperature overnight in the dark. Particulate matter was removed by centrifugation. The supernatant was diluted with an equal volume of 25 mM potassium phosphate buffer (pH 6.5) and applied to PBE 94 ( $1.6 \times 8$  cm) equilibrated with the same buffer. Gradient elution with KCl (0 to 0.5 M; 300 mL) resolved DNS-lisinopril from dansic acid which eluted at 0.1 and 0.15 M KCl, respectively. TLC of the DNS-lisinopril fraction on Silica Gel 60 (Merck, FRG) in butanol:acetic acid:water (4:1:1) revealed a single fluorescent spot ( $R_F$  0.73) with no evidence for contamination by DNS-OH ( $R_F$  0.62). Identification of DNS-lisinopril was based on TLC analysis [Silica Gel 60; chloroform:methanol:17% ammonia (2:2:1)] before and after acid hydrolysis. Treatment of the sample with 6.1 N HCl at 110° overnight yielded a ninhydrin-positive spot with an  $R_F$  corresponding to that of a standard proline solution treated in the same manner. Fluorescence excitation and emission spectra of the dansylation product are given in Fig. 2. The concentration of DNS-lisinopril in the PBE 94 eluate was calculated using  $E_{330} = 4 \text{ mM}^{-1} \text{ cm}^{-1}$  reported for similar dansylated compounds [28]. The eluate was used without further treatment.

**Kinetic measurements.** Assays were conducted at 35°, in 0.1 M HEPES buffer (pH 8) containing 0.3 M NaCl, 0.1 mM ZnCl<sub>2</sub> and 0.25 to 1.5 mM FAPGG. [The assay mixture also contained 5% (v/v) methanol coming from the substrate stock solution. However,

the methanol content was found not to affect the kinetic results.] Reactions were initiated by the addition of enzyme (*ca.* 0.3  $\mu$ g protein/mL) and monitored through the change in absorbance at 345 nm. Activity was calculated using  $\Delta E = 0.517 \text{ mM}^{-1} \text{ cm}^{-1}$  [29].

All inhibition experiments were conducted at  $[I]_{\text{total}}$  in significant excess over  $[E]_{\text{total}}$ , in order to avoid inhibitor depletion during the approach to the steady state\*; the concentration of ACE in the system lay in the subnanomolar range, as deduced from activity observed at 25° (0.01 U/mL), the specific activity reported for pure enzyme (72–146 U/mg) and a molecular mass of 135–185 kDa [15, 22, 31, 32]. The lowest inhibitor concentrations used were 3 nM (lisinopril) and 6 nM (DNS-lisinopril).

## RESULTS AND DISCUSSION

In the substrate concentration range covered, in the absence of inhibitor, bovine lung ACE exhibited Michaelis–Menten kinetics, with  $K_m$  (FAPGG) = 0.26 mM.

**Inhibition by lisinopril.** Progress curves for FAPGG hydrolysis in the absence and presence of lisinopril are given in Fig. 3. In analogy to its effect on rabbit lung ACE [21–24], lisinopril acted as a slow-binding inhibitor of the bovine lung enzyme. Final steady-state velocities were reached on the minute time scale. The approach to the steady state was a pseudo first order process [Fig. 3b, plotted according to [33], substituting  $(A_t - A_{ss})$  for  $([P]_{ss} - [P]_t)$ ]. The variation of the observed rate constant for inhibition with  $[I]$  (not shown) was in keeping with Scheme I and Equation 1 relating to it [22].

$$k_{\text{obsd}} = \frac{(k_2 + k_{-2})[I] + k_{-2}K_i(1 + [S]/K_m)}{[I] + K_i(1 + [S]/K_m)} \quad (1)$$

Estimated values for the various parameters (with  $K_m = 0.26$  mM) were:  $K_i$ , 3.3 nM;  $k_2$ ,  $4.3 \times 10^{-2} \text{ sec}^{-1}$  and  $k_{-2}$ ,  $1.7 \times 10^{-3} \text{ sec}^{-1}$ , in qualitative agreement with values reported in the comprehensive study on rabbit lung ACE [22].  $K_i^*$ , the overall dissociation constant ( $K_i k_{-2}/(k_2 + k_{-2})$ ), was 0.12 nM.

On the other hand, Dixon plots of steady-state velocities as a function of  $[I]$  (Fig. 4) did not conform to a simple competitive model. The steady-state equation for Scheme I (Eq. 2) requires that Dixon plots have slopes directly proportional to  $[S]^{-1}$ . Such was not the case; a 6-fold increase

$$V_{\text{steady state}} = \frac{V_{\max}[S]}{K_m(1 + [I]/K_i^*) + [S]} \quad (2)$$

\* Failure to observe this condition complicates kinetic analyses in all phases of the inhibition: (a) the initial, slow phase, if any, has to be treated as a second order process rather than a pseudo first order one, i.e. allowance has to be made not only for time-dependent changes in available enzyme concentration, but also for time-dependent changes in free  $[I]$ ; and (b) the steady state is no longer described by conventional rate equations; complex equations [30] must be used, precluding graphical diagnosis of inhibition type.

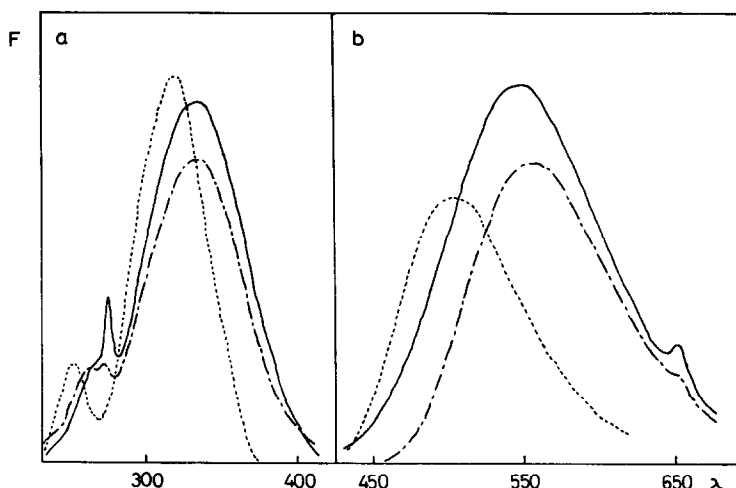


Fig. 2. Fluorescence spectra of DNS-lisinopril. (a) Excitation spectrum; emission measured at 550 nm. (b) Emission spectrum; excitation at 327 nm. (Spectra for DNS-6-aminocaproic acid (—) and DNS-OH (---) are included for comparison.)

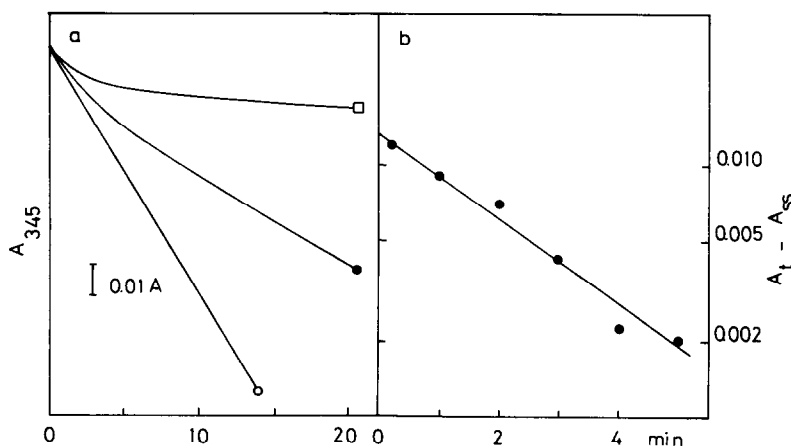
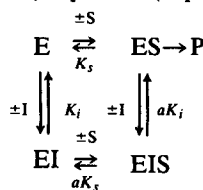


Fig. 3. Effect of lisinopril on FAPGG hydrolysis by bovine lung ACE. (a) Progress curves at 0 (○), 3 (●) and 10 (□) nM lisinopril.  $[S] = 1.5$  mM. (b) Semilogarithmic replot of the data at 3 nM inhibitor.

in substrate concentration reduced the slope by a factor of 2, pointing to inhibition of the linear mixed type. A minimal mechanism which could account for the observed steady-state behavior is given in Scheme II. The data were analyzed according to the (rapid equilibrium) equation (Eq. 3)



Scheme II

$$v^{-1} = \frac{(1 + aK_s/[S])[I]}{aK_i V_{\max}} + \frac{(1 + K_s/[S])}{V_{\max}} \quad (3)$$

for this scheme. Taking  $K_s = K_m = 0.26$  mM,  $K_i$  and  $aK_i$  [overall dissociation constants incorporating factors from any  $EI(EIS)$  to  $EI^*(EIS^*)$  transitions that may be taking place] were calculated to be 0.7 and 1.1 nM, respectively.

**Inhibition by DNS-lisinopril.** The data for lisinopril inhibition (Fig. 4) showed considerable scatter, arising from the need to use  $[I] \gg [E]$ , which resulted in reduction of steady-state activities almost to the limit of detection. The experiments were repeated with DNS-lisinopril, where significant residual activity was observed at the high inhibitor concentrations required. The data (Fig. 5) pointed to the same pattern of steady-state inhibition as deduced for lisinopril. The values for  $K_i$  and  $aK_i$  obtained using Equation 3 were 4.7 and 14 nM, respectively. A preliminary study of the approach to steady-state

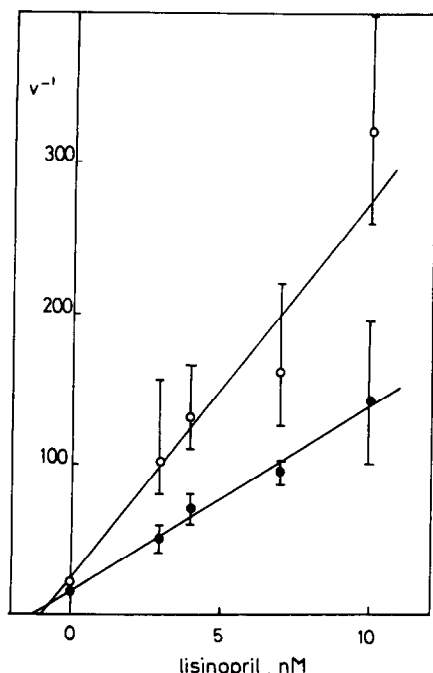


Fig. 4. Dixon plot for steady-state inhibition of FAPGG hydrolysis by lisinopril.  $[S] = 0.25$  (○) and  $1.5$  mM;  $v$  is in units of  $\Delta A_{345}/10$  min. (The points are averages of at least three determinations. The bars indicate the range of values obtained.)

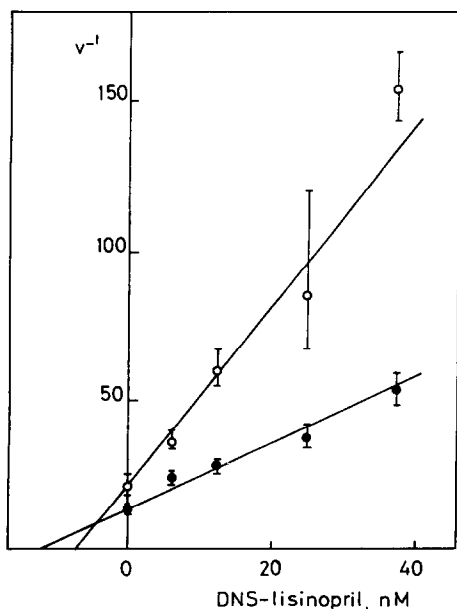


Fig. 5. Dixon plot for steady-state inhibition of FAPGG hydrolysis by DNS-lisinopril.  $[S] = 0.25$  (○) and  $1.5$  mM. (The points are averages of at least three determinations. The bars indicate the range of values obtained.)

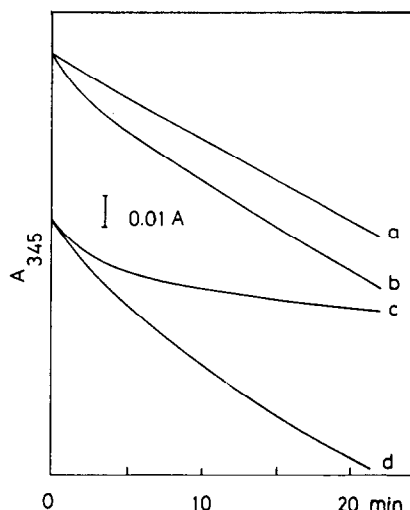


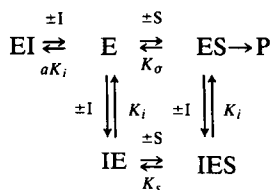
Fig. 6. Dependence of progress curves for FAPGG hydrolysis on  $[S]$  and the identity of inhibitor. Inhibition by  $25$  nM DNS-lisinopril (a) and  $3$  nM lisinopril (b) at  $[S] = 1.5$  mM and inhibition by  $25$  nM DNS-lisinopril (c) at  $[S] = 0.25$  mM. [The progress curve (d) in the absence of inhibitor has been included to give an estimate of the nonlinearity arising from substrate depletion at  $0.25$  mM  $S$  and thereby to highlight the slow-onset inhibition by DNS-lisinopril at this substrate concentration.]

activity, on the other hand, repeatedly revealed differences between the two inhibitors. When progress curves were compared at lisinopril and DNS-lisinopril concentrations which yielded similar  $v^{+1}$  (steady-state)/ $v^{-1}$  ratios, only a marginal presteady-state period was observed with DNS-lisinopril at  $[S] = 1.5$  mM, as opposed to the definite curvature in the lisinopril traces (Fig. 6, curves a and b). At  $[S] = 0.25$  mM, the progress curve for DNS-lisinopril inhibition (Fig. 6, curve c) assumed the expected features of slow-onset inhibition. With reference to Scheme II, these observations imply that both EI and EIS undergo inhibitor-induced isomerization. In the case of DNS-lisinopril, isomerization of EIS must be faster than isomerization of EI. In contrast, qualitative assessment of the inhibition by lisinopril at high and low  $S$  suggests that EI and EIS must isomerize at comparable rates.

In conclusion, the data presented provide evidence against lisinopril as a conventional tight-binding *competitive* inhibitor of ACE. Both E and ES appear to bind I and to undergo conformational changes. The simplest model which fits the steady-state kinetic data is one involving a single I-binding site (Scheme II). The occupation of this site adversely affects substrate binding, at the same time rendering the enzyme incapable of carrying out its catalytic function.

A variant of this model [34] involves two mutually exclusive I-binding sites (Scheme III, Eq. 4). Binding at one of the sites is competitive with substrate binding. Binding at the alternative site gives rise to the noncompetitive component of the observed inhibition. Schemes II and III are kinetically

indistinguishable. Therefore, the data presented provide no evidence in favor of one mechanisms over the other. Nevertheless,



Scheme III

$$v^{-1} = \frac{(c + K_s/[S])[I]}{cKV_{\max}} + \frac{(1 + K_s/[S])}{V_{\max}} \quad (4)$$

$$(c = a/(1 + a))$$

Scheme III is relevant, especially with reference to the finding that ACE harbors two homologous [18, 19] and active [35] domains in its structure and a recent reappraisal of the stoichiometry of lisinopril binding [36]. Thus, it is highly likely that lisinopril and DNS-lisinopril can bind to both of the active domains. Binding to the C-terminal domain (corresponding to the formation of EI in Scheme III) would account for the competitive component of the inhibition observed, since it is this domain that accounts for 90% of ACE activity towards synthetic substrates [35]. Binding to the N-terminal domain (formation of IE as distinct from EI), on the other hand, would be reflected in a change in  $k_{\text{cat}}$ , i.e. the efficiency of substrate turnover at the C-terminal active site. A definite conclusion regarding the alternative modes of inhibition must await further studies on the intramolecular dynamics of ACE.

## REFERENCES

- Ondetti MA and Cushman DW, Angiotensin-converting enzyme inhibitors: Biochemical properties and biological actions. *CRC Crit Rev Biochem* **16**: 381–411, 1984.
- Patchett AA and Cordes EH, The design and properties of *N*-carboxyalkyldipeptide inhibitors of angiotensin-converting enzyme. *Adv Enzymol* **57**: 1–84, 1985.
- Allan G, Cambridge D, Hardy GW and Follenfant MJ, BW A575C, a chemically novel agent with angiotensin converting enzyme inhibitor and  $\beta$ -adrenoreceptor-blocking properties. *Br J Pharmacol* **90**: 609–615, 1987.
- Negwer M, Internationale kurzbezeichnungen für pharmazeutisch verwendete substanzen. *Pharm Ind* **51**: 365–375, 1989.
- Strittmatter SM and Snyder SH, Characterization of angiotensin converting enzyme by [ $^3\text{H}$ ]captopril binding. *Mol Pharmacol* **29**: 142–148, 1986.
- Shapiro R and Riordan JF, Critical lysine residue at the chloride binding site of angiotensin converting enzyme. *Biochemistry* **22**: 5315–5321, 1983.
- Bünning P, Holmquist B and Riordan JF, Substrate specificity and kinetic characteristics of angiotensin converting enzyme. *Biochemistry* **22**: 103–110, 1983.
- Harris RB and Wilson IB, Glutamic acid is an active site residue of angiotensin I-converting enzyme. Use of the Lossen rearrangement for identification of dicarboxylic acid residues. *J Biol Chem* **258**: 1357–1362, 1983.
- Harris RB, Ohlsson JT and Wilson IB, Inhibition and affinity chromatography of human serum angiotensin converting enzyme with cysteinyl-proline derivatives. *Arch Biochem Biophys* **206**: 105–112, 1981.
- Bünning P, Holmquist B and Riordan JF, Functional residues at the active site of angiotensin converting enzyme. *Biochem Biophys Res Commun* **83**: 1442–1449, 1978.
- Cushman DW, Cheung HS, Sabo EF and Ondetti MA, Design of potent competitive inhibitors of angiotensin-converting enzyme. Carboxyalkanoyl and mercaptoalkanoyl amino acids. *Biochemistry* **16**: 5484–5491, 1977.
- Das M and Soffer RL, Pulmonary angiotensin-converting enzyme. Structural and catalytic properties. *J Biol Chem* **250**: 6762–6768, 1975.
- Cheung HS and Cushman DW, Inhibition of homogeneous angiotensin-converting enzyme of rabbit lung by synthetic venom peptides of *Bothrops jararaca*. *Biochim Biophys Acta* **293**: 451–463, 1973.
- Lanzillo JJ, Stevens J, Dasarathy Y, Yotsumoto H and Fanburg BL, Angiotensin-converting enzyme from human tissues: Physicochemical, catalytic, and immunological properties. *J Biol Chem* **260**: 14938–14944, 1985.
- Bull HG, Thornberry NA and Cordes EH, Purification of angiotensin-converting enzyme from rabbit lung and human plasma by affinity chromatography. *J Biol Chem* **260**: 2963–2972, 1985.
- Schullek JR and Wilson IB, The binding of zinc to angiotensin-converting enzyme. *Arch Biochem Biophys* **265**: 346–350, 1988.
- Bicknell R, Holmquist B, Lee FS, Martin MT and Riordan JF, Electronic spectroscopy of cobalt angiotensin converting enzyme and its inhibitor complex. *Biochemistry* **26**: 7291–7297, 1987.
- Soubrier F, Alhenc-Gelas F, Hubert C, Allegrini J, John M, Tregar G and Corvol P, Two putative active centers in human angiotensin I converting enzyme revealed by molecular cloning. *Proc Natl Acad Sci USA* **85**: 9386–9390, 1988.
- Bernstein KE, Martin BM, Edwards AS and Bernstein EA, Mouse angiotensin-converting enzyme is a protein composed of two homologous domains. *J Biol Chem* **264**: 11945–11951, 1989.
- Shai S-Y, Langford KG, Martin BM and Bernstein KE, Genomic DNA 5' to the mouse and human angiotensin-converting enzyme genes contains two distinct regions of conserved sequence. *Biochem Biophys Res Commun* **167**: 1128–1133, 1990.
- Reynolds CH, Kinetics of inhibition of angiotensin converting enzyme by captopril and by enalapril diacid. *Biochem Pharmacol* **33**: 1273–1276, 1984.
- Bull HG, Thornberry NA, Cordes MHJ, Patchett AA and Cordes EH, Inhibition of rabbit lung angiotensin-converting enzyme by  $N^{\alpha}$ -[(S)-1-carboxy-3-phenylpropyl]-L-alanyl-L-proline and  $N^{\alpha}$ -[(S)-1-carboxy-3-phenylpropyl]-L-lysyl-L-proline. *J Biol Chem* **260**: 2952–2962, 1985.
- Shapiro R and Riordan JF, Inhibition of angiotensin converting enzyme: Dependence on chloride. *Biochemistry* **23**: 5234–5240, 1984.
- Goli UB and Galardy RE, Kinetics of slow, tight-binding inhibitors of angiotensin converting enzyme. *Biochemistry* **25**: 7136–7142, 1986.
- Riordan JF, Harper JW and Martin M, The catalytic mechanism of angiotensin converting enzyme and related zinc enzymes. *J Cardiovasc Pharmacol* **8** (Suppl 10): S29–S34, 1986.
- Harper JW, Shapiro R and Riordan JF, Observation of a chloride-dependent intermediate during catalysis by angiotensin converting enzyme using radiationless energy transfer. *Biochemistry* **26**: 1284–1288, 1987.
- Bradford M, A rapid and sensitive method for the quantitation of microgram quantities of protein utilizing

- the principle of protein-dye binding. *Anal Biochem* **72**: 248–254, 1976.
28. Penny GS and Dyckes DF, Interaction of dansylated peptidyl chloromethanes with trypsin, chymotrypsin, elastase and thrombin. *Biochemistry* **19**: 2888–2894, 1980.
29. Holmquist B, Bünning P and Riordan JF, A continuous spectrophotometric assay for angiotensin converting enzyme. *Anal Biochem* **95**: 540–548, 1979.
30. Morrison JF and Walsh CT, The behavior and significance of slow binding inhibitors. *Adv Enzymol* **61**: 201–301, 1988.
31. Bünning P, Kleemann SG and Riordan JF, Essential residues in angiotensin converting enzyme: Modification with 1-fluoro-2,4-dinitrobenzene. *Biochemistry* **29**: 10488–10492, 1990.
32. Chen Y-NP and Riordan JF, Identification of essential tyrosine and lysine residues in angiotensin converting enzyme: Evidence for a single active site. *Biochemistry* **29**: 10493–10498, 1990.
33. Neet KE and Ainslie GR Jr, Hysteretic enzymes. *Methods Enzymol* **64**: 192–226, 1980.
34. Segel IH, *Enzyme Kinetics*, pp. 176–178. Wiley-Interscience, New York, 1975.
35. Wei L, Alhenc-Gelas F, Corvol P and Clauser E, The two homologous domains of human angiotensin I-converting enzyme are both catalytically active. *J Biol Chem* **266**: 9002–9008, 1991.
36. Ehlers MRW and Riordan JF, Angiotensin-converting enzyme: Zinc- and inhibitor-binding stoichiometries of the somatic and testis isozymes. *Biochemistry* **30**: 7118–7126, 1991.